

# Analysis of Mean Waiting Time for Delivery of a Message in Mobile Multi-Hop Networks

Keisuke NAKANO<sup>†a)</sup>, Member, Kazuyuki MIYAKITA<sup>†</sup>, Student Member, Akira OTSUKA<sup>††</sup>, Member, Masakazu SENGOKU<sup>†</sup>, Fellow, and Shoji SHINODA<sup>†††</sup>, Fellow, Honorary Member

**SUMMARY** Analysis of waiting time to deliver a message  $M$  from a source  $S$  to a destination  $D$  is deeply related to connectivity analysis, which is an important issue in fundamental studies of mobile multi-hop networks. In [1], we compared the mean waiting times of two methods to deliver  $M$  with the mean value of the minimum waiting time. The mean minimum waiting time was obtained by computer simulation because theoretical analysis of this mean is not easy, although another two methods were analyzed theoretically. In this paper, we propose an approximate method to theoretically analyze the mean minimum waiting time in a one-dimensional street network, and show that this method gives a good approximation of the mean minimum waiting time. Also, we consider shadowing and change of directions of mobile nodes at intersections as negative factors arising in two-dimensional street networks. We extend the above method to compute the mean minimum waiting time considering these factors, and discuss how the mean minimum waiting time is affected by these factors.

**key words:** mobile multi-hop network, connectivity, mobility, epidemic routing

## 1. Introduction

In mobile multi-hop networks [2], [3], each node has capabilities of direct communication and relaying. These capabilities enable mobile nodes to construct a multi-hop path between mobile nodes. Mobile nodes can exchange information if there is a multi-hop path between them; however, mobile nodes sometimes encounter a situation where there is no multi-hop path between them because positions of mobile nodes are generally random and the transmitting range is finite. Therefore, connectivity analysis is important for understanding behavior of mobile multi-hop networks [4].

As a measure of connectivity, the probability that there is at least one path between a source  $S$  and a destination  $D$  is often used. As another measure for mobile multi-hop networks, [1], [5] use the mean of the waiting time from the time when a request for transmission of a message  $M$  destined for  $D$  arrives at  $S$  to the time when  $D$  receives  $M$ . Assume that  $M$  arrives at  $S$  at  $t = \tau_1$  and that  $M$  is received by  $D$  at  $\tau_2$ . The waiting time  $\tau_2 - \tau_1$  depends on how  $M$  is delivered from  $S$  to  $D$ . Also, from the viewpoint of applications,

there are applications that accept a long waiting time, such as data collection through a sensor network, where  $S$ ,  $D$ , and  $M$  correspond to a sensor node, a data center, and data observed by  $S$ , respectively. Here, we assume that sensors and relay nodes in the sensor network can be mobile nodes. In mobile multi-hop networks for such applications, the mean waiting time can be an appropriate measure of connectivity, and it depends on the method to send  $M$  to  $D$ . Then, in [1], the following three methods were compared.

**Method 1:** If there is at least a multi-hop path between  $S$  and  $D$  at  $\tau_1$ , then  $S$  sends  $M$  to  $D$  immediately. Otherwise,  $S$  keeps searching a multi-hop path to  $D$  by a certain routing protocol until the routing protocol finds a multi-hop path between  $S$  and  $D$  expecting that a multi-hop path will appear between  $S$  and  $D$  because mobility of relay nodes changes topology with time. Finally,  $S$  sends  $M$  to  $D$  through this multi-hop path. In [1], the routing protocol was assumed to be an ideal one that can always notice appearance of a connected multi-hop path between  $S$  and  $D$ . This method reflects the basic behavior of ordinary ad-hoc routing protocols.

**Method 2:** Epidemic routing [6] delivers  $M$  to  $D$  by making mobile nodes move  $M$  closer to  $D$ , and can be realized in various manners like the proposed algorithm in [6]. In [1], we compared the simplest epidemic routing, which does not use multi-hop transmission, with Method 1 to explore how mobility of nodes affects the mean waiting time. The simplest epidemic routing is called Method 2. In Method 2,  $S$  directly sends  $M$  to all mobile nodes in its communication range. It is expected that some of these nodes approach  $D$  as time passes and may finally enter the communication range of  $D$ . If this actually occurs,  $M$  can be delivered to  $D$  directly from mobile nodes having  $M$ . In actual situations, we need some protocol to realize Method 2. To do this, for example,  $S$  has to periodically broadcast  $M$  to mobile nodes in its communication range, and mobile nodes having  $M$  have to periodically check whether they are in the communication range of  $D$  by exchanging control signals. Although there may be various ways to realize Method 2, here we assume an ideal situation where  $S$  can always notice that there are mobile nodes in its communication range and mobile nodes having  $M$  can always notice that they enter the communication range of  $D$ . Method 2 does not use multi-hop transmission and utilizes only capability of mobility to move  $M$  closer to  $D$ . Then, we can intuitively see that the waiting time becomes long if Method 2 is used;

Manuscript received December 26, 2008.

Manuscript revised April 9, 2009.

<sup>†</sup>The authors are with the Dept. of Information Engineering, Niigata University, Niigata-shi, 950-2181 Japan.

<sup>††</sup>The author is with Mitsubishi Electric Corporation, Kamakura-shi, 247-8501 Japan.

<sup>†††</sup>The author is with the Dept. of Electrical, Electronic and Communication Engineering, Chuo University, Tokyo, 112-8551 Japan.

a) E-mail: nakano@ie.niigata-u.ac.jp  
DOI: 10.1587/transfun.E92.A.2236

however, Method 2 can sometimes deliver M to D faster than Method 1 for a small density of nodes as shown in [1].

**Method 3:** This method is a combination of Methods 1 and 2. If there is at least a multi-hop path between S and D at  $\tau_1$ , then S sends M to D immediately like Method 1. Otherwise, S sends M to all mobile nodes that have multi-hop paths from S, and mobile nodes that received M repeatedly distribute M to other nodes in the same manner. For example, such distribution of M is done by flooding. Finally, M is delivered to D. Here, we assume that scheduling of flooding is ideally executed and neglect delay caused by collision of packets for simplifying analysis and clarifying how the change of topology with time affects the waiting time. Hence, Method 3 minimizes the waiting time in this case.

Let  $T_{w,1}$ ,  $T_{w,2}$  and  $T_{w,3}$  be  $\tau_2 - \tau_1$  for Methods 1, 2 and 3, respectively, and let  $E(\cdot)$  be the mean value of  $\cdot$ . In [1],  $E(T_{w,1})$ ,  $E(T_{w,2})$  and  $E(T_{w,3})$  were analyzed and characterized relatively in a one-dimensional mobile multi-hop network consisting of a fixed source S, a fixed destination D, and pedestrians walking at a constant velocity  $v$  along a street. Note that S, D, and pedestrians correspond to a sensor node, a data center, and mobile relay nodes, respectively, if the network is used as a sensor network. We analyzed these mean waiting times assuming that positions of nodes are randomly decided and using probabilistic properties of relative positions of nodes.

As shown in [1], Methods 2 and 3 outperform Method 1 for a small density of nodes and Method 1 is no longer effective in such a situation because  $E(T_{w,1})$  rapidly increases as the density of nodes decreases. Therefore, we pay attention to situations where the density of nodes is small and the mean waiting time is large. Based on this policy, we neglect short delays caused in a queue of packets or in transmissions of packets through direct links or multi-hop paths for simplifying analysis. Also, as mentioned, we assume an ideal situation where S, D, and mobile nodes can always notice existence of nodes in their communication ranges and appearance of multi-hop paths. From these assumptions,  $T_{w,1}$ ,  $T_{w,2}$  and  $T_{w,3}$  in [1] are considered as lower bounds of the waiting times of Methods 1, 2 and 3 in actual situations, respectively.

Furthermore, comparison between  $E(T_{w,1})$ ,  $E(T_{w,2})$  and  $E(T_{w,3})$  gives some insights to know how differently mobility of nodes affects the mean waiting time as mentioned in [1]. In Method 1, mobility helps nodes to construct a connected multi-hop path by changing the topology of the network. This capability of mobility is called Capability 1 in [1]. In Method 2, mobility helps nodes to move M closer to D. This capability of mobility is called Capability 2 in [1]. Method 3 maximally utilizes these capabilities of mobility to minimize the waiting time. We showed that  $E(T_{w,2}) > E(T_{w,1}) \approx E(T_{w,3})$  if the density of nodes is large, and that  $E(T_{w,1}) > E(T_{w,2}) \approx E(T_{w,3})$  if the density of nodes is sufficiently small. This means that Capability 1 works sufficiently well without any assistance from Capability 2 if the density of nodes is large, and that the reverse is true if the density of nodes is sufficiently small. From these results,

we can well understand how  $E(T_{w,1})$ ,  $E(T_{w,2})$  and  $E(T_{w,3})$  behave differently due to different effects of mobility.

In [1],  $E(T_{w,1})$  and  $E(T_{w,2})$  were theoretically analyzed. However,  $E(T_{w,3})$  was obtained by computer simulation although a theoretical lower bound was given because theoretical analysis is not easy, as mentioned in [1]. In [7], an approximate method to analyze the mean waiting time of Method 3 in a one-dimensional vehicle network was recently proposed.

Although a one-dimensional street network on a line was assumed in [1], street networks usually include corners and intersections. As a result, shadowing occurs at corners and mobile nodes can change their directions at intersections. If shadowing occurs at a corner between S and D, Method 1 cannot construct any multi-hop paths between them. If a mobile node having M does not move toward D due to a change of direction at an intersection, Method 2 cannot deliver M to D. It is expected that these negative factors also affect Method 3 and increase the mean minimum waiting time; however,  $E(T_{w,3})$  was not theoretically analyzed in these situations.

With this as background, in this paper, we propose an approximate method to compute  $E(T_{w,3})$  theoretically. We analyze  $E(T_{w,3})$  in three models, called Models 1, 2 and 3. Model 1 is almost the same model as that used in [1]. In Model 1, mobile nodes are pedestrians moving along a line. In Model 2, we assume that there are some corners along a street and shadowing occurs around the corners. In Model 3, we assume that there are intersections along a street and mobile nodes change their directions at intersections. We show that the approximate methods well describe  $E(T_{w,3})$  in these models and show how shadowing and the change of direction affect  $E(T_{w,3})$ . Although Model 1 and the approximate method derived for Model 1 are similar to the network model and the approximate method in [7], the equations for Model 1 derived in this paper are different from those in [7], and [7] does not consider effects of shadowing and the change of direction of mobile nodes on the waiting time.

## 2. Mean Waiting Time in Model 1

### 2.1 Definitions and Assumptions

First, we propose an approximate method to compute  $E(T_{w,3})$  theoretically in Model 1. The following are definitions and assumptions made in Model 1. The assumptions are essentially the same as those in [1] except for  $A_1$ .

**A1:** Suppose that all nodes including a source S and a destination D are on a line. In [1], we considered transmission of a message M from S to D assuming that S and D were fixed nodes. To simplify analysis, in this paper, we assume that a request of transmission of M arrives at a mobile node moving toward D at  $t = \tau_1$ . Denote this node by S. Assume that D is fixed and that other nodes are mobile nodes. As mentioned, we consider that S is a mobile sensor node that moves with a pedestrian and D is a fixed data center. Let  $x(n, t)$  be the coordinate of a node  $n$  at time  $t$  on the

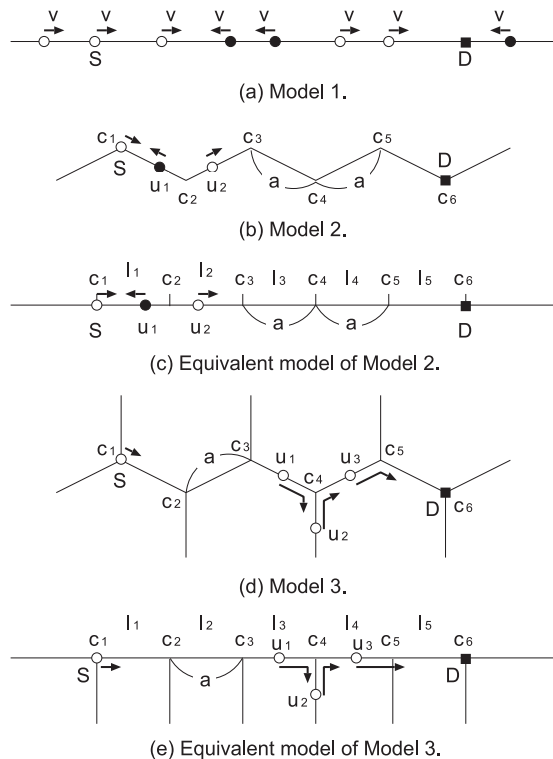


Fig. 1 Models.

line. Let  $L$  be the distance from  $S$  to  $D$  at  $\tau_1$ . Suppose that  $x(S, \tau_1) = 0$ , and that  $x(D, t) = L$  for all  $t$  because  $D$  is stationary. Define again that  $\tau_2$  is the moment when  $D$  receives  $M$ .

**A2:** Assume that a mobile node is a pedestrian walking along the line at a constant velocity  $v$  independently of other nodes without changing direction. As represented in Fig. 1(a), mobile nodes moving left (in the direction from  $D$  to  $S$ ) are represented by black nodes and those moving right (in the direction from  $S$  to  $D$ ) are represented by white nodes. As mentioned, we consider that these mobile nodes comprise a mobile multi-hop path along which  $M$  is transmitted or move  $M$  closer to  $D$ .

**A3:** Let  $N_b$  and  $N_w$  be the sets of mobile nodes moving left and those moving right, respectively. Denote a mobile node of  $N_b$  by  $b_i$ , where  $i$  is an integer such that  $x(b_i, t) < x(b_{i+1}, t)$  for all  $i$  and all  $t$ . Denote a mobile node of  $N_w$  by  $w_j$ , where  $j$  is an integer such that  $x(w_j, t) < x(w_{j+1}, t)$  for all  $j$  and all  $t$ . Note that the above definition of  $w_j$  is slightly different from that in [1].

**A4:** Assume that the distributions of nodes of  $N_b$  and  $N_w$  obey Poisson distributions of intensity  $\frac{\lambda}{2}$  at the initial moment  $t = 0$ , respectively. Note that the same distributions are observed at time  $t > 0$  because mobile nodes move independently from other nodes [8].

**A5:** Assume that there exists a wireless link between two nodes if the distance between them is not longer than  $r$ , where  $r$  is a positive constant and  $r < L$ . Otherwise, there is no link between them.

**A6:** Let  $N_M(t)$  be the set of nodes having  $M$  at time  $t$ .

Let  $N'_M(t)$  be the set of nodes that do not have  $M$  at time  $t$ . Then,  $S \in N_M(\tau_1)$ . Let  $n_h^t$  be the node whose coordinate is the largest in  $N_M(t)$ . Let  $n_{h,w}^t$  be the node of  $N_w$  whose coordinate is the largest in  $N_M(t)$ . Let  $X(t)$  and  $X_w(t)$  be the coordinates of  $n_h^t$  and  $n_{h,w}^t$  at  $t$ , respectively.

**A7:** Suppose that  $u_1 \in N_M(\tau_a)$  and  $\{u_2, u_3, \dots, u_k\} \subset N'_M(\tau_a)$ , where  $k \geq 2$ , and that  $x(u_1, \tau_a) < x(u_2, \tau_a) < \dots < x(u_k, \tau_a)$ . Topology of the network changes with time under the above assumption. Suppose that  $u_1$  becomes connected to  $\{u_2, u_3, \dots, u_k\}$  due to the change of topology at  $\tau_b = \tau_a + \Delta\tau$ , where  $\Delta\tau$  is a small constant, that is,  $x(u_2, \tau_b) - x(u_1, \tau_b) \leq r$ ,  $x(u_3, \tau_b) - x(u_2, \tau_b) \leq r$ , ...,  $x(u_k, \tau_b) - x(u_{k-1}, \tau_b) \leq r$ . Assume that  $M$  is forwarded from  $u_1$  to  $u_2, \dots, u_k$  simultaneously at  $\tau_b$  without delay.

**A8:** If an interval has no node and the length of this interval is greater than  $r$ , we call this interval a gap. If an interval has no node of  $N_b$  and the length of this interval is greater than  $r$ , we call this interval a gap of  $N_b$ . A gap of  $N_w$  is defined in the same manner.

## 2.2 Related Work

In [7], an approximate method to compute  $E(T_{w,3})$  in a vehicle network similar to Model 1 was recently proposed. This method computes  $E(T_{w,3})$  by dividing the distance between  $S$  and  $D$  by the average message transfer velocity. The average message transfer velocity was computed from  $t_{DTN}^{(i)}$  and  $S_{m-hop}$ , defined in [7]. As can be seen from the following subsections, this concept is similar to our analysis in Model 1, and  $t_{DTN}^{(i)}$  and  $S_{m-hop}$  correspond to  $T_{walk}$  and the mean of  $X_{fwd,w}$ , which are defined in the following subsections, respectively. In [7],  $t_{DTN}^{(i)}$  and  $S_{m-hop}$  are derived by dividing a street into vehicle slots with length  $l$ , which is the length of each vehicle, and using the probability that there exists at least one vehicle in a slot, and it is assumed that  $t_{DTN}^{(i)}$  obeys an exponential distribution. The validity of this analysis is shown by comparing numerical results of this analysis with simulation results. In [7], it is assumed that the velocity of mobile node is a random variable. This assumption is more complicated than that in this paper; however, only a line network was considered in [7] while this paper considers effects of shadowing and inflow and outflow of mobiles at intersections in Models 2 and 3.

Although the outline of our approximate method to compute  $E(T_{w,3})$  is similar to that of [7], we derive the mean value of  $X_{fwd,w}$  differently from [7] and derive the density function of  $T_{walk}$  from properties of clumps as explained below while these properties are not used in [7]. As a result, in this paper, the density function of  $T_{walk}$  is obtained as a function different from an exponential distribution, and other probabilities and mean values not used in [7] are derived. Also, the final form of  $E(T_{w,3})$  is different from that in [7]. Furthermore, as can be understood later, our analysis in Model 1 can be simply extended to those in Models 2 and 3 because the final form of  $E(T_{w,3})$  in Model 1 is suitable to extension to analyses in Models 2 and 3.

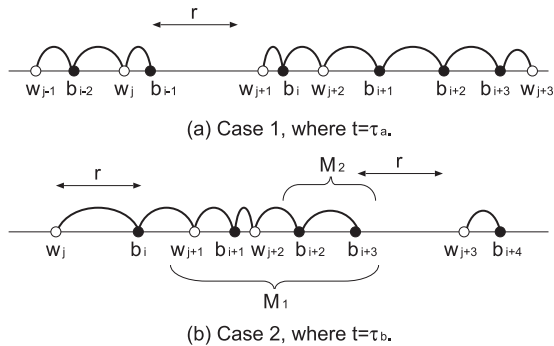


Fig. 2 Examples of forwarding.

### 2.3 Mean Progress of M in One Forwarding

In Model 1, we can move M closer to D by forwarding M through a multi-hop path. Even if forwarding is impossible, M approaches D as mobile nodes of  $N_w$  having M walk toward D. We call a time interval in which forwarding is impossible a “walking period.” After a walking period, forwarding is done and the next walking period begins. We consider how much M is made closer to D by one forwarding to compute  $E(T_{w,3})$ . To do this, we consider the progress of M assuming that the distance to D is very long. Although this progress can be measured by  $X(t)$ , we consider  $X_w(t)$  as the progress of M for simplifying analysis. In the following, we first explain the reason we consider  $X_w(t)$  as the progress of M, and second explain how much M is made closer to D by one forwarding.

Figure 2(a) shows a situation at  $t = \tau_a$  in a walking period where  $\{w_{j-1}, b_{i-2}, w_j, b_{i-1}\} \subset N_M(\tau_a)$  and  $\{b_i, \dots, b_{i+3}, w_{j+1}, \dots, w_{j+3}\} \subset N'_M(\tau_a)$ . Because there is a gap between  $b_{i-1}$  and  $w_{j+1}$ , M cannot be forwarded to any nodes of  $N'_M(\tau_a)$ . To forward M to nodes of  $N'_M(\tau_a)$  after  $\tau_a$ , we have to wait until the distance between  $w_j$  and  $b_i$  becomes equal to  $r$ . In general, if a walking period ends at  $t$ , then  $n_h^{t-\Delta t}$  must be in  $N_w$  and there must be a node of  $N_b$  at  $x(n_h^{t-\Delta t}, t) + r$  at  $t$ , where  $\Delta t$  is a small positive constant. Therefore, nodes of  $N_b$  cannot be sources to forward M to mobile nodes which do not have M.

Figure 2(b) shows a situation where the above walking period ends. Suppose that  $t = \tau_b$  and that  $n_h^{\tau_b-\Delta t} = w_j$ . Then, the distance between  $w_j$  and  $b_i$  is equal to  $r$  as mentioned. M is forwarded from  $w_j$  to  $b_i$ ,  $w_{j+1}$ ,  $b_{i+1}$ ,  $w_{j+2}$ ,  $b_{i+2}$  and  $b_{i+3}$ . Then,  $n_h^{\tau_b} = b_{i+3}$  and  $n_{h,w}^{\tau_b} = w_{j+2}$ . Because a node of  $N_b$  cannot be a source of the next forwarding after  $\tau_b$  as mentioned, the source node of the next forwarding is  $w_{j+2}$ . Consider  $X(t) - X_w(t)$ , which is the distance between  $n_h^t$  and  $n_{h,w}^t$  at  $t$ . Define that  $\Delta X_{fwd}$  is the mean of  $X(t) - X_w(t)$  given that a walking period ends at  $t$ . After  $\tau_b$ ,  $X(t) - X_w(t)$  decreases and finally becomes equal to 0 because  $n_h^t$  and  $n_{h,w}^t$  approach if  $n_h^t \in N_b$ . Note again that  $n_h^t \in N_b$  cannot forward M to nodes  $N'_M(\tau_b)$  until  $n_h^t$  and  $n_{h,w}^t$  come to the same position. Consequently, we can see that the nodes in the right of  $n_{h,w}^t$  cannot essentially contribute to the progress of M.

Therefore, we consider  $X_w(t)$  as the progress of M instead of  $X(t)$  for simplifying analysis of  $E(T_{w,3})$ .

Consider the situation in Fig. 2(b) again. Using the notations in Fig. 2(b), we consider the mean progress of M by one forwarding. Let  $M_1$  be the number of nodes that are on the right of  $b_i$  and have at least a multi-hop path to  $b_i$  as shown in Fig. 2(b). Denote these  $M_1$  nodes by  $u_1, u_2, \dots, u_{M_1}$ , such that  $x(u_1, \tau_b) < x(u_2, \tau_b) < \dots < x(u_{M_1}, \tau_b)$ . Let  $u_0$  be  $b_i$ . Suppose that  $u_{M_1-M_2+1} \in N_b$ ,  $u_{M_1-M_2+2} \in N_b, \dots, u_{M_1-1} \in N_b$  and  $u_{M_1} \in N_b$ . Let  $X_{fwd}$  be the distance between  $w_j$  to  $u_{M_1}$ . Let  $X_{fwd,w}$  be the distance between  $w_j$  to  $u_{M_1-M_2}$  given that  $M_1 > M_2$ , namely there is at least a node of  $N_w$  in  $u_1, \dots, u_{M_1}$ . Then, we mainly pay attention to  $E(X_{fwd,w})$  as the mean progress of M in one forwarding because it corresponds to the increase of  $X_w(t)$ . As shown in Appendix A,

$$E(X_{fwd,w}) = \frac{e^{\lambda r}}{\lambda} - \frac{r}{e^{\lambda r} - 1}. \quad (1)$$

For reference, we have

$$\Delta X_{fwd} = E(X_{fwd} | M_1 > M_2) - E(X_{fwd,w}) \leq r \quad (2)$$

as shown in Appendix A. Namely,  $\Delta X_{fwd}$  is at most  $r$ , and this property supports the above assumption from another point of view that the progress of M realized by nodes of  $N_b$  does not essentially contribute to the progress of M.

As mentioned, in the approximate method in [7],  $S_{m-hop}$  corresponds to  $E(X_{fwd,w})$ . As can be seen from the above equations and the equations in [7], the derivation and final form of  $E(X_{fwd,w})$  are different from those of  $S_{m-hop}$ .

### 2.4 Density Function of the Length of a Walking Period

In this subsection, we consider the length of a walking period that begins at  $\tau_c$ . Denote this length by  $T_{walk}$ . As mentioned,  $T_{walk}$  corresponds to  $t_{DTN}^{(i)}$  in [7]. There is a big difference between [7] and this paper in the derivation of the density function of  $T_{walk}$ . In the analysis in [7],  $t_{DTN}^{(i)}$  is assumed to obey an exponential distribution. As explained in the following, however,  $T_{walk}$  depends on the distance between adjacent nodes of  $N_w$  and the lengths of connected components consisting of nodes of  $N_b$ , which are called clumps in the following. Due to this dependence, it is not easy to prove that  $T_{walk}$  obeys an exponential distribution. In the following, we derive the density function of  $T_{walk}$ , which is not expressed as an exponential distribution, although some approximations are used.

First, we explain the concept of a clump, which is deeply related to  $T_{walk}$ . Consider nodes on the right of a node  $u_k$  at  $t$ . Denote these nodes by  $u_{k+1}, u_{k+2}, \dots$  and suppose that  $x(u_k, t) < x(u_{k+1}, t) < x(u_{k+2}, t) < \dots$ . If  $x(u_{k+1}, t) - x(u_k, t) \leq \alpha$ ,  $x(u_{k+2}, t) - x(u_{k+1}, t) \leq \alpha, \dots, x(u_{k+l}, t) - x(u_{k+l-1}, t) \leq \alpha$  and  $x(u_{k+l+1}, t) - x(u_{k+l}, t) > \alpha$ , where  $\alpha$  is a constant, then the interval  $[x(u_k, t), x(u_{k+l}, t) + \alpha]$  is called a clump, which begins from  $u_k$ . For a clump consisting of nodes distributed according to a Poisson distribution of intensity  $\beta$ , the density function of the length of

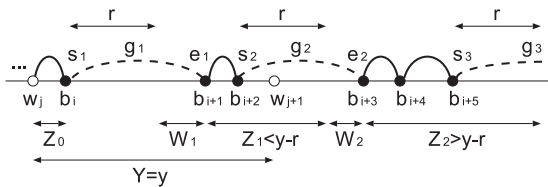


Fig. 3 Variables to define  $T_{walk}$ .

a clump has been given in [9] and the mean of the clump length is  $\frac{e^{\alpha\beta}-1}{\beta}$ . Also, in [9], it has been mentioned that the exponential distribution with the mean  $\frac{e^{\alpha\beta}-1}{\beta}$  can be used as an approximation to the distribution of the length of a clump for a large  $\beta$ . In the following, we compute the density of  $T_{walk}$  using these properties.

Let  $C$  be an event where there is a gap between  $w_j$  and  $w_{j+1}$  at  $\tau_c$ . We show an example of the situation at  $\tau_c$  in Fig.3, and explain  $T_{walk}$  using some variables as shown in this figure. Suppose that  $w_j$  corresponds to  $n_{h,w}^{\tau_c}$ . Let  $Y$  be a random variable identical to the distance between  $w_j$  and  $w_{j+1}$ . Suppose that  $Y = y$  at  $\tau_c$ , where  $y$  is a positive constant. Here,  $Y > r$  because of the gap as mentioned. Denote by  $g_k$   $k$ th gap of  $N_b$  on the right of  $w_j$  at  $\tau_c$ , where  $k = 1, 2, \dots$ . Let  $s_k$  and  $e_k$  be coordinates of black nodes at both ends of  $g_k$ , where  $s_k < e_k$ . Then,  $g_k$  corresponds to an interval  $(s_k, e_k)$ , and the black nodes at  $e_{k-1}$  and  $s_k$  have a connected path consisting of black nodes between them for all  $k$ . Let  $Z_k$  and  $W_k$  be  $s_{k+1} - e_k + r$  and  $e_k - s_k - r$ , respectively, where  $k = 1, 2, \dots$ . Let  $Z_0$  be  $s_1 - x(w_j, \tau_c)$ . Let  $Z_{sum}$  and  $W_{sum}$  be  $\sum_{k=1}^{m-1} Z_k$  and  $\sum_{k=1}^m W_k$ , respectively, if  $Z_1 < y - r, Z_2 < y - r, \dots, Z_{m-1} < y - r$  and  $Z_m \geq y - r$ . Then, we have

$$T_{walk} = \frac{Z_0 + Z_{sum} + W_{sum}}{2v} \quad (3)$$

because if  $Z_1 < y - r, Z_2 < y - r, \dots, Z_{m-1} < y - r$  and  $Z_m \geq y - r$ , then the black nodes between  $e_m$  and  $s_{m+1}$  can connect  $w_j$  and  $w_{j+1}$  when the distance between the black node that is at  $e_m$  at time  $\tau_c$  and  $w_j$  becomes equal to  $r$ .

By letting  $\alpha$  and  $\beta$  be  $r$  and  $\frac{\lambda}{2}$ , respectively, we can see that  $Z_k$  for  $k \geq 1$  corresponds to the length of a clump consisting of nodes of  $N_b$  from the definitions of  $Z_k$  and a clump, where  $\alpha = r, \beta = \frac{\lambda}{2}$ , and the mean of  $Z_k$  is  $\frac{e^{\frac{\lambda r}{2}} - 1}{\frac{\lambda}{2}}$ . For simplicity, we assume that  $Z_k$  approximately obeys an exponential distribution with the mean  $\frac{e^{\frac{\lambda r}{2}} - 1}{\frac{\lambda}{2}}$  as mentioned. Based on this assumption, by letting  $\alpha$  and  $\beta$  be  $y - r$  and  $\Lambda = \frac{\lambda}{e^{\frac{\lambda(y-r)}{2}} - 1}$ , we can see that  $Z_{sum} + y - r$  again means the length of a clump with the mean  $\frac{e^{\Lambda(y-r)} - 1}{\Lambda}$  if  $Z_1 < y - r, Z_2 < y - r, \dots, Z_{m-1} < y - r$  and  $Z_m \geq y - r$ . We can again assume that  $Z_{sum} + y - r$  obeys an exponential distribution of intensity  $\frac{\Lambda}{e^{\Lambda(y-r)} - 1}$ . Because we need the density of  $Z_{sum}$ , for simplicity, we roughly compute the density of  $Z_{sum}$  as an exponential distribution of intensity  $\Lambda_Z$ , where  $\Lambda_Z = \left\{ \frac{e^{\Lambda(y-r)} - 1}{\Lambda} - (y - r) \right\}^{-1}$ .

Also,  $W_{sum}$  is the sum of exponential random variables. Suppose that  $M_3$  is a random variable such that  $Z_1 < y - r,$

$Z_2 < y - r, \dots, Z_{M_3-1} < y - r$  and  $Z_{M_3} \geq y - r$ . Then, the density function of  $W_{sum}$ , denoted by  $f_{W_{sum}}(w)$  is as follows:

$$\begin{aligned} f_{W_{sum}}(w) &= \sum_{m_3=1}^{\infty} f_{W_{sum}}(w|M_3 = m_3)P(M_3 = m_3) \\ &= \Lambda_W e^{-\Lambda_W w} \end{aligned} \quad (4)$$

where  $f_{W_{sum}}(w|M_3 = m_3) = \frac{(\frac{\Lambda_W}{2})^{m_3}}{(m_3-1)!w} e^{-\frac{\Lambda_W}{2}w}$  because  $W_k$  obeys an exponential distribution of  $\frac{\Lambda}{2}$ ,  $P(M_3 = m_3) = (1 - e^{-\Lambda(y-r)})^{m_3-1} e^{-\Lambda(y-r)}$  and  $\Lambda_W = \frac{\lambda}{2} e^{-\Lambda(y-r)}$ .

Here,  $Z_0$  is identical to the  $X(\tau_c) - X_w(\tau_c)$ , and the mean of this length is identical to  $\Delta X_{fwd}$  and is at most  $r$  as mentioned. For simplicity, therefore, we approximate  $Z_0$  as  $E(Z_0) = \Delta X_{fwd}$ . Then, from this approximation and the above equations, we have

$$\begin{aligned} f_{T_{walk}}(t|Y = y) &= \int_0^{2vt - E(Z_0)} 2v f_{Z_{sum}}(2vt - E(Z_0) - w) f_{W_{sum}}(w) dw \\ &= \frac{2v \Lambda_W \Lambda_Z \{e^{-\Lambda_Z(2vt - E(Z_0))} - e^{-\Lambda_W(2vt - E(Z_0))}\}}{\Lambda_W - \Lambda_Z} \end{aligned} \quad (5)$$

if  $t \geq \frac{E(Z_0)}{2v}$  and is equal to 0 otherwise. Let  $f_Y(y)$  be the density function of  $Y$ . Then,

$$f_{T_{walk}}(t) = \int_{-\infty}^{\infty} f_{T_{walk}}(t|Y = y) f_Y(y|C) dy. \quad (6)$$

For unconditioning of Eq. (5), we use  $f_Y(y|C)$  given in Appendix B. Although unfortunately we cannot obtain the closed form of  $f_{T_{walk}}(t)$ , we numerically compute  $f_{T_{walk}}(t)$ .

## 2.5 Velocity of Movement of M and Mean Waiting Time

To compute  $E(T_{w,3})$ , we use  $V_M$ , which is the mean progress of M carried by nodes of  $N_w$  per unit time. Define that  $B$  is an event where S cannot forward M to any nodes of  $N_w$  before the distance from S to D becomes equal to  $r$ . Denote  $V_M$  by  $V_{M,B}$  if  $B$  occurs, and by  $V_{M,\bar{B}}$  otherwise. If  $B$  occurs, then S does not have multi-hop paths to any nodes of  $N_w$  at  $\tau_1$  and  $T_{walk}$  is longer than  $\frac{L-r}{v}$ . Then

$$P(B) = P(C)P\left(T_{walk} > \frac{L-r}{v}\right), \quad (7)$$

where  $P(C)$  is given in Appendix B and  $P\left(T_{walk} > \frac{L-r}{v}\right)$  can be computed from Eq. (6). If  $B$  occurs, then M is carried by S without multi-hop transmission to nodes of  $N_w$ . Hence,

$$V_{M,B} = v. \quad (8)$$

In general, M is moved closer to D by walking of  $n_{h,w}^t$  and forwarding from  $n_{h,w}^t$  alternately. If  $B$  does not occur, we pay attention to this property and compute  $V_{M,\bar{B}}$  as the ratio of the mean progress of M in one cycle of walking and forwarding to the mean length of a walking period, and approximately compute  $V_{M,\bar{B}}$  as follows:

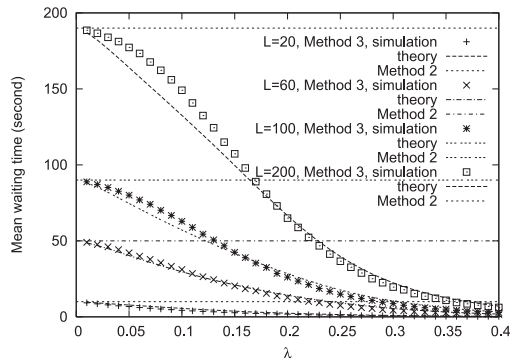


Fig. 4 Numerical results of  $E(T_{w,3})$  in Model 1.

$$V_{M,\bar{B}} = \frac{vE(T_{walk}|T_{walk} \leq \frac{L-r}{v}) + E(X_{fwd,w})}{E(T_{walk}|T_{walk} \leq \frac{L-r}{v})} \quad (9)$$

because  $T_{walk} \leq \frac{L-r}{v}$  if  $B$  does not occur. Using  $V_M$ , we roughly compute  $E(T_{w,3})$  as

$$E(T_{w,3}) = P(B) \frac{L-r}{V_{M,B}} + \{1 - P(B)\} \frac{L-r}{V_{M,\bar{B}}}. \quad (10)$$

The reason we divide  $L-r$  by  $V_{M,B}$  or  $V_{M,\bar{B}}$  is that  $D$  can receive  $M$  if the distance between  $D$  and  $M$  is  $r$ . Note that although [7] uses a concept similar to Eq. (10), [7] does not consider two events  $B$  and  $\bar{B}$  separately. This classification will be utilized in the analyses of  $E(T_{w,3})$  in Models 2 and 3.

We show the numerical results of  $E(T_{w,3})$  obtained by the above method in Fig. 4 together with the simulation results. To obtain the simulation results, we use the same method as used in [1]. Here,  $r = 10$  m and  $v = 1$  m/sec. Although we use some approximations, the numerical results agree well with the simulation results. From these results, we can confirm the validity of the approximate method. We can also confirm that  $E(T_{w,3})$  decreases as  $\lambda$  increases and that  $E(T_{w,3})$  increases as  $L$  increases.

For reference, we also showed  $E(T_{w,2})$ , which is the mean of the maximum waiting time of epidemic routing while  $E(T_{w,3})$  is the mean of the minimum waiting time of epidemic routing. To compute  $E(T_{w,2})$ , we assume that  $S$  delivers  $M$  to  $D$  by itself. Then,  $E(T_{w,2})$  is  $\frac{L-r}{v}$ . We can confirm that Method 3 can move  $M$  faster than Method 2. Their difference becomes smaller as  $\lambda$  decreases, and finally Method 3 is almost identical to Method 2 for a small  $\lambda$ . As shown in this result, by comparing the mean waiting times of Methods 2 and 3, we can understand how forwarding decreases the mean waiting time for a given  $\lambda$ . We can see that the difference increases as  $L$  increases, and forwarding demonstrates its ability for a large  $L$ .

### 3. Mean Waiting Time in Model 2

The approximate method provided in the preceding section enables us to theoretically compute  $E(T_{w,3})$  in a one-dimensional street network. As a next step, we consider the same problem in two-dimensional street networks. First, we

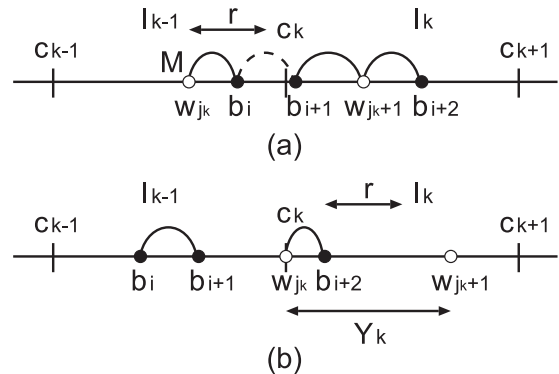


Fig. 5 Relation between  $w_{jk}$  and  $w_{jk+1}$  in Model 2.

consider effects of shadowing at corners along a street. Suppose that a street is surrounded by buildings and that there are some corners on the street. Then, a mobile node may not be able to communicate with a mobile node beyond the corner. Here, we assume that mobile nodes having a corner between them cannot directly communicate with each other even if the distance between them is not longer than  $r$ . We try to compute  $E(T_{w,3})$  with this assumption together with the assumptions in Sect. 2. We call the model considered here Model 2. Here, we consider  $n_c + 1$  corners. We assume that  $S$  is at a corner  $c_1$  at  $\tau_1$  and  $D$  is at a corner  $c_{n_c+1}$ . Suppose that corners  $c_2, c_3, \dots, c_{n_c}$  exist between  $S$  and  $D$  as shown in Fig. 1(b). In this example, nodes  $u_1$  and  $u_2$  cannot directly communicate with each other due to shadowing at  $c_2$ . Denote that  $I_k$  be the interval between  $c_k$  and  $c_{k+1}$ . Suppose that the length of each interval is a constant  $a$ , where  $a \geq r$ . Other than the above assumptions and definitions, we use the assumptions and definitions made in Model 1. To do this, we assume the street in Model 2 as a straight line in which there are  $n_c + 1$  corners at a constant interval  $a$  and shadowing occurs at each corner as shown in Fig. 1(c). From this assumption, we can define  $N_b$ ,  $N_w$  and the coordinates of nodes in the same manner as in Model 1.

In Model 2,  $M$  cannot be forwarded from a node on  $I_k$  to another node on  $I_{k+1}$  because of shadowing. Then,  $M$  is delivered to a new interval always by walking of a node of  $N_w$  having  $M$ . We try to roughly compute  $E(T_{w,3})$  in Model 2 assuming that flow of  $M$  in  $I_k$  is almost identical to that in Model 1, where  $L = a$ . Suppose that  $w_{jk}$  is in  $I_{k-1}$  and has  $M$  and that  $w_{jk+1}$  is not in  $I_{k-1}$  and does not have  $M$  as shown in Fig. 5(a). In this figure,  $w_{jk+1}$  cannot receive  $M$  because  $b_i$  and  $b_{i+1}$  are not connected owing to shadowing at  $c_k$ . Assume that  $w_{jk}$  arrives at  $c_k$  at  $\tau_a$  as shown in Fig. 5(b). Let  $Y_k$  be the distance between  $w_{jk}$  and  $w_{jk+1}$ . Let  $C_k$  be an event where there is no path between  $w_{jk}$  and  $w_{jk+1}$  at  $\tau_a$ . For example,  $C_k$  occurs in Fig. 5(b). Note that  $C_k$  includes an event where there is a corner between  $w_{jk}$  and  $w_{jk+1}$ .

In Model 1, we implicitly suppose a situation where cycles of walking and forwarding are repeated. In Model 2, however, we sometimes meet a situation where a walking period never ends. Such a situation occurs if  $Y_k$  is longer than  $a$ . Considering such a situation separately, we define

that  $T_{walk,k}$  is the length from  $\tau_a$  to the end of a walking period that begins at  $\tau_a$  given that  $C_k$  occurs, and  $Y_k \leq a$ . Define that  $B_k$  is an event where  $w_{j_k}$  cannot forward M to  $w_{j_{k+1}}$  before  $w_{j_k}$  leaves  $I_k$ . Then,  $B_k$  is the union of the following events:

- $Y_k > a$ ,
- $Y_k \leq a$ ,  $C_k$  and  $T_{walk,k} > \frac{a-r}{v}$ .

Here, we make an assumption that is not needed in Model 1. In Model 2, if  $Y_k > a$ , then a walking period never ends after M enters  $I_k$  as mentioned, and  $B_k, B_{k+1}, \dots$  must occur. From this fact, we assume that  $P(B_{k+1}|B_k) = 1$  to simplify analysis. Then, for  $k = 2, 3, \dots, n_c - 1$ ,

$$P(B_k) = P(B_{k-1}) + P(\overline{B_{k-1}}) \left\{ P(Y_k > a) + P(Y_k \leq a)P(C_k|Y_k \leq a)P\left(T_{walk,k} > \frac{a-r}{v}\right) \right\}. \quad (11)$$

$P(B_1)$  and  $P(B_{n_c})$  are slightly different from this equation because S exists at  $c_1$  initially and there is no effect of shadowing in  $I_{n_c}$ . Then,

$$P(B_1) = P(Y_1 > a) + P(Y_1 \leq a)P(C_1|Y_1 \leq a) \times P\left(T_{walk,1} > \frac{a-r}{v}\right), \quad (12)$$

$$P(B_{n_c}) = P(B_{n_c-1}) + P(\overline{B_{n_c-1}})P(C_{n_c}) \times P\left(T_{walk,n_c} > \frac{a-r}{v}\right). \quad (13)$$

To compute  $P(Y_k > a)$  and  $P\left(T_{walk,k} > \frac{a-r}{v}\right)$ , we give the density functions of  $Y_k$  and  $T_{walk,k}$  in Appendix C. Also, we give  $P(C_k|Y_k \leq a)$  in Appendix C. By using equations in Appendix C, we can compute  $P(B_k)$  for  $k = 1, 2, \dots, n_c$ .

Denote  $V_M$  by  $V_{M,B_k}$  if  $B_k$  occurs, and by  $V_{M,\overline{B_k}}$  otherwise. Then, we roughly compute  $V_{M,B_k}$  and  $V_{M,\overline{B_k}}$  in the same manner as in Model 1 as follows:

$$V_{M,B_k} = v, \quad (14)$$

$$V_{M,\overline{B_k}} = \frac{vE(T_{walk,k}|T_{walk,k} \leq \frac{a-r}{v}) + E(X_{fd,w})}{E(T_{walk,k}|T_{walk,k} \leq \frac{a-r}{v})}. \quad (15)$$

Here, we compute  $E(X_{fd,w})$  by Eq. (1) to simplify computation of  $V_{M,\overline{B_k}}$ . To compute  $V_{M,\overline{B_k}}$ , we use the density function of  $T_{walk,k}$  represented in Appendix C.

We define that  $T_{w,3,k}$  is the length of an interval from the time when M enters  $I_k$  to the time when M enters  $I_{k+1}$  for  $k = 2, \dots, n_c - 1$ . We define that  $T_{w,3,1}$  is the length of an interval from  $\tau_1$  to the time when M enters  $I_2$  and that  $T_{w,3,n_c}$  is the length of an interval from the time when M enters  $I_{n_c}$  to the time when D receives M. We compute  $T_{w,3,k}$  as follows: For  $k = 1, \dots, n_c - 1$ ,

$$E(T_{w,3,k}) = P(\overline{B_k}) \left\{ \frac{a - E(Y_{k+1,1})}{V_{M,\overline{B_k}}} + \frac{E(Y_{k+1,1})}{V_{M,B_k}} \right\} + P(B_k) \frac{a}{V_{M,B_k}}. \quad (16)$$

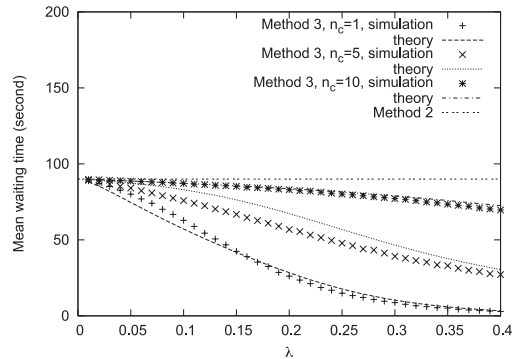
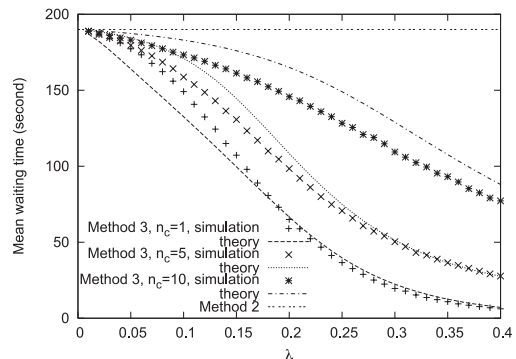
(a)  $L = 100\text{m}$ .(b)  $L = 200\text{m}$ .

Fig. 6 Numerical results of  $E(T_{w,3})$  in Model 2 for  $n_c = 1, 5$  and  $10$ .

$$E(T_{w,3,n_c}) = P(\overline{B_{n_c}}) \frac{a-r}{V_{M,B_{n_c}}} + P(B_{n_c}) \frac{a-r}{V_{M,B_{n_c}}}. \quad (17)$$

For  $k = 1, \dots, n_c - 1$ ,  $n_{h,w}^t$  must walk in the last part of  $I_k$  due to shadowing; therefore, we assume in Eq. (16) that the mean length of this “walking” part is  $E(Y_{k+1,1})$ , which is given in Appendix C.

Finally, we can compute  $E(T_{w,3})$  as

$$E(T_{w,3}) = \sum_{k=1}^{n_c} E(T_{w,3,k}). \quad (18)$$

Numerical results of  $E(T_{w,3})$  in Model 2 for  $n_c = 1, 5$  and  $10$  are represented in Fig. 6 together with simulation results. We assume that  $L = 100\text{m}$  and  $L = 200\text{m}$  in Figs. 6(a) and (b), respectively. Note that the results for  $n_c = 1$  mean that those when shadowing never occurs. For reference, we also showed  $E(T_{w,2})$ , which is  $\frac{L-r}{v}$ .

From these results, we can confirm that the numerical results well describe characteristics of  $E(T_{w,3})$  although there is a difference between the numerical and simulation results in some cases because of approximations used in the analysis. In the analysis, we assumed that  $P(B_{k+1}|B_k) = 1$ . This approximation means that  $B_{k+1}$  strongly depends on  $B_k$ . We consider that the tendency of the numerical results of  $E(T_{w,3})$  well describes that of the simulation results due to this assumption of dependence; however, the exact value of  $P(B_{k+1}|B_k)$  is not equal to 1. Therefore, the above approximation of  $P(B_{k+1}|B_k)$  is one factor that sometimes causes a difference between the numerical results and the simulation

results. The more accurate analysis of  $P(B_{k+1}|B_k)$  is considered as a future problem. These figures show that the mean waiting time rapidly increases as shadowing occurs more frequently, and it increases as  $\lambda$  decreases. We can see that Method 3 can move  $M$  faster than Method 2 even if shadowing occurs. As explained in the analysis of  $E(T_{w,3})$  in Model 2, the velocity of  $M$  decreases and becomes equal to the velocity of walking if a large gap appears between nodes. Due to such a negative effect of shadowing,  $E(T_{w,3})$  approaches  $E(T_{w,2})$  as  $\lambda$  decreases.

Although Method 1 cannot send  $M$  from  $S$  to  $D$  if shadowing occurs between  $S$  and  $D$  as mentioned, Method 3 can deliver  $M$  to  $D$  even if shadowing occurs. This feature is an advantage of Method 3 other than its quickness while Method 3 is faster than Method 1 in nature.

#### 4. Mean Waiting Time in Model 3

In Model 2, we considered effects of shadowing at corners on the message delivery. At corners of streets, there is another factor that may increase the mean waiting time. If there is an intersection at a corner, a mobile node sometimes changes its direction. The change of direction of a mobile node with  $M$  may increase the waiting time if this node does not move toward  $D$ . We consider such a situation, called Model 3, and extend the analysis in Model 2 to consider negative effects of the change of direction at intersections on the mean waiting time.

For Model 3, we consider the network depicted in Fig. 1(d). In this network, there are intersections, each of which is connected to three streets. We assume that shadowing occurs between each pair of streets. For example, in Fig. 1(d), shadowing occurs between  $u_1$  and  $u_2$ , between  $u_2$  and  $u_3$ , and between  $u_3$  and  $u_1$ . To simplify explanation, we transform the network in Fig. 1(d) to the network in Fig. 1(e).

Consider the network in Fig. 1(e). Assume that a mobile node never turns back and turns each corner after selecting its direction from among the two directions. We assume that flows of mobile nodes are as represented in Fig. 7 and Table 1. We assume the density of nodes moving along a route from  $\gamma_1$  to  $\gamma_2$  is  $\frac{\lambda(1-P_{turn})}{2}$ , where  $0 \leq P_{turn} \leq 1$ , as shown in this table. In the same manner, we show the density of nodes moving along other routes in Table 1. From this assumption, the density of nodes moving from  $\gamma_1$  to  $\gamma_4$  is  $\frac{\lambda}{2}$  and that moving from  $\gamma_4$  to  $\gamma_1$  is also  $\frac{\lambda}{2}$ . Therefore, if we observe the flow of mobile nodes moving along  $I_1, I_2, \dots, I_{n_c}$ , this flow is almost the same as that in Model 2 except for the fact that some nodes leave or enter  $I_1, I_2, \dots, I_{n_c}$  in Model 3. Hence, by comparing Models 2 and 3, we can observe effects of the change of direction of nodes. In the following, we consider  $E(T_{w,3})$  in Model 3 using the same definitions of variables by considering a sequence of  $I_1, I_2, \dots, I_{n_c}$  in Model 3 as the street in Model 2.

If  $Y_k > a$  in Model 2, then  $V_M = v$  because the topology of the network consisting of nodes of  $N_w$  does not change. On the other hand, in Model 3, a mobile node turns at

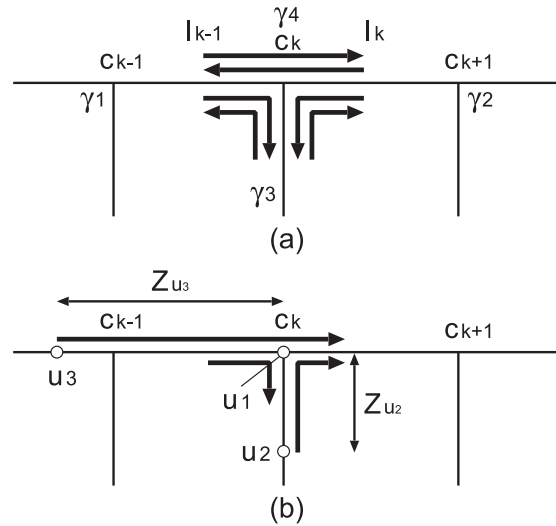


Fig. 7 Flows of mobiles in Model 3.

Table 1 Density of nodes of each flow.

Direction	Density of nodes
$\gamma_1 \rightarrow \gamma_2$	$\frac{\lambda(1-P_{turn})}{2}$
$\gamma_1 \rightarrow \gamma_3$	$\frac{\lambda P_{turn}}{2}$
$\gamma_2 \rightarrow \gamma_1$	$\frac{\lambda(1-P_{turn})}{2}$
$\gamma_2 \rightarrow \gamma_3$	$\frac{\lambda P_{turn}}{2}$
$\gamma_3 \rightarrow \gamma_1$	$\frac{\lambda P_{turn}}{2}$
$\gamma_3 \rightarrow \gamma_2$	$\frac{\lambda P_{turn}}{2}$

each corner as mentioned. Then, topology of the network changes with time more dynamically than those in Model 2. Even if  $Y_k > a$  in Model 3,  $Y_{k+1}$  can be smaller than or equal to  $a$ . This is a difference between Models 2 and 3. Therefore, although we assume that  $P(B_{k+1}|B_k) = 1$  in Model 2, we eliminate this assumption in Model 3 and suppose that

$$P(B_k) = P(Y_k > a) + P(Y_k \leq a) \times P(C_k | Y_k \leq a) P\left(T_{walk,k} > \frac{a-r}{v}\right) \quad (19)$$

for  $k = 1, 2, \dots, n_c - 1$ , and

$$P(B_{n_c}) = P(C_{n_c}) P\left(T_{walk,n_c} > \frac{a-r}{v}\right). \quad (20)$$

We compute the probabilities in the right terms of these equations in the same manner as in Model 2.

Also, a mobile node having  $M$  does not always move toward the direction of  $D$ . In this case,  $M$  must be carried along a redundant path. For example, in Fig. 7(b),  $u_1$ , which has  $M$  and moves toward  $D$ , changes its direction at  $c_k$ . In this example,  $u_2$  receives  $M$  from  $u_1$  and moves toward  $D$ , and  $u_3$ , which has  $M$  and follows  $u_1$ , also moves toward  $D$ . Then,  $u_2$  and  $u_3$  can play the same role as  $u_1$ . However, the length of an interval of time when  $u_1$  arrives at  $c_k$  to the time when  $u_2$  or  $u_3$  arrives at  $c_k$  must be added to the waiting time in this case. This detour of  $M$  is another difference between Models 2 and 3.

To take into account these effects, we consider Fig. 7 again. Suppose that  $u_1$ , which has  $M$ , is at the corner  $c_k$  and that there is no node that has  $M$  in  $I_k, I_{k+1}, \dots$ . Suppose that  $u_2$  moves toward  $c_{k+1}$  through  $c_k$  after passing  $u_1$  and that  $u_3$ , which follows  $u_1$ , moves toward  $c_{k+1}$  through  $c_k$ . Then,  $u_2$  must receive  $M$  from  $u_1$ . For simplicity, we assume that  $u_3$  also receives  $M$  before arriving at  $c_k$  from nodes that received  $M$  although  $u_3$  may not be able to receive  $M$ . Then,  $u_2$  and  $u_3$  can move  $M$  in  $I_k$  by walking or forwarding instead of  $u_1$ . Hence, we add the mean length of an interval from the time when  $u_1$  arrives at  $c_k$  to the time when  $u_2$  or  $u_3$  arrives at  $c_k$  into Eqs. (16) and (17) after substituting Eqs. (19) and (20) into these equations, and use the result of this addition as  $E(T_{w,3,k})$  in Model 3. Let  $Z_{u_2}$  and  $Z_{u_3}$  be the distances from  $u_1$  to  $u_2$  and  $u_3$  when  $u_1$  is at  $c_k$ , respectively.  $Z_{u_2}$  is an exponential random variable with intensity  $\frac{\lambda P_{turn}}{2}$ , and  $Z_{u_3}$  is an exponential random variable with intensity  $\frac{\lambda(1-P_{turn})}{2}$  as can be seen from Table 1. Then, we approximately compute  $E(T_{w,3})$  in Model 3 as

$$E(T_{w,3}) = E(T_{w,3,1}) + \sum_{k=2}^{n_c} \left\{ E(T_{w,3,k}) + P_{turn} \frac{E(\min(Z_{u_2}, Z_{u_3}))}{v} \right\}, \quad (21)$$

where  $E(T_{w,3,k})$  and  $E(T_{w,3,n_c})$  are computed by Eqs. (16) and (17), respectively, after substituting  $P(B_k)$  for Model 3 into these equations and  $E(\min(Z_{u_2}, Z_{u_3})) = \frac{2}{\lambda}$ .

We show the numerical results of  $E(T_{w,3})$  in Model 3 for  $P_{turn} = 0, 0.25, 0.5, 0.75$  and  $1$  in Fig. 8 together with simulation results. We assume that  $L = 100$  m and  $L = 200$  m in Figs. 8(a) and (b), respectively, and that  $n_c = 5$ . From the results, we can see that the numerical results agree with the simulation results. If we compare Fig. 6 and Fig. 8, we can see that, in Model 3, the numerical results agree with the simulation results better than in Model 2. One reason for this result is as follows:  $E(T_{w,3,k})$  deeply depends on  $E(T_{w,3,k-1})$  in Model 2 as explained to compute  $P(B_k)$  in Model 2, and difficulty in analysis of this dependence causes the difference between numerical results and simulation results in Model 2. On the other hand, in Model 3, the distributions of nodes in  $I_{k-1}$  and  $I_k$  are less dependent than those in Model 2 because of inflow and outflow of nodes at  $c_k$ . As a result, a simple approximation analysis in Model 3 provides better results than in Model 2.

From Fig. 8,  $E(T_{w,3})$  increases as  $\lambda$  decreases.  $E(T_{w,3})$  increases as  $P_{turn}$  increases for the following reasons. Here, a situation where  $P_{turn} = 0$  means that every node moves along a line from  $c_1$  to  $c_{n_c+1}$  without changing its direction; namely this situation is identical to Model 2. A situation where  $P_{turn} = 1$  means that there is no node moving along a line from  $c_1$  to  $c_{n_c+1}$  without changing its direction; namely this situation causes detours of  $M$  at intersections most frequently. Then, we can observe the above characteristic.

In Fig. 8, we plot  $E(T_{w,2})$  given that  $S$  successfully delivers  $M$  to  $D$  by itself although Method 2 cannot always deliver  $M$  to  $D$  in Model 3 because  $S$  does not always arrive at  $D$  because of change of direction. Namely,  $E(T_{w,2}) = \frac{L-r}{v}$ .

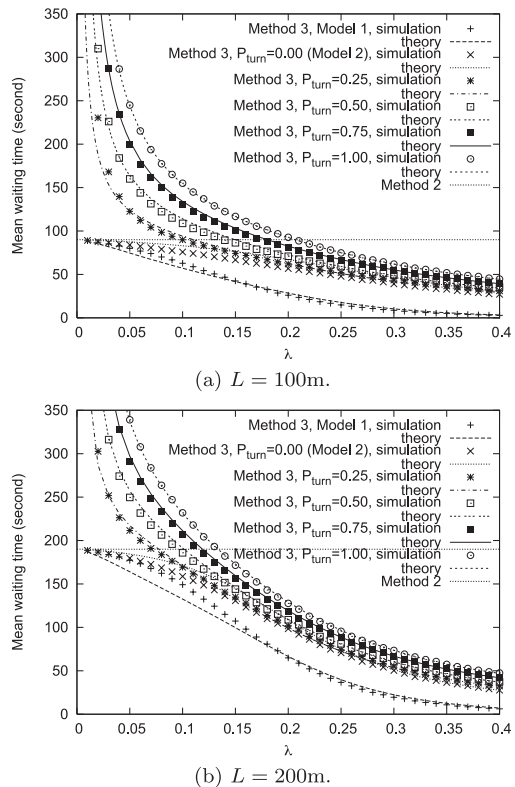


Fig. 8 Numerical results of  $E(T_{w,3})$  in Model 3 for  $P_{turn} = 0, 0.25, 0.5, 0.75$  and  $1.0$ , where  $n_c = 5$ .

In this case, the difference between  $E(T_{w,3})$  for  $P_{turn} > 0$  and that for  $P_{turn} = 0$  corresponds the increase of  $E(T_{w,3})$  caused by the detours of  $M$ . Due to the increase of  $E(T_{w,3})$  caused by the detours,  $E(T_{w,3})$  is sometimes greater than  $\frac{L-r}{v}$ . As mentioned, however, Method 3 can deliver  $M$  to  $D$  with the mean waiting time depicted in Fig. 8 as opposed to Method 2, which cannot always deliver  $M$  to  $D$ . This property is also an advantage of Method 3.

## 5. Discussions on Results in Models 2 and 3

In the analysis of  $E(T_{w,3})$  in Model 2, we assumed that  $B_{k+1}$  strongly depends on  $B_k$  for  $k = 1, 2, \dots, n_c - 1$ . Furthermore, we approximately set  $P(B_{k+1}|B_k)$  to be 1 as an extreme approximation. However, the numerical results well describe the tendency of  $E(T_{w,3})$ . Hence, we can confirm the validity of our analysis. Then, this result indicates that in Model 2, forwarding rarely occurs in intervals  $I_{k+1}, I_{k+2}, \dots$  once forwarding does not occur in  $I_k$  because of the dependence between  $B_k$  and  $B_{k+1}$ . Therefore, we can see that the dependence between  $B_k$  and  $B_{k+1}$  is an important factor that should be considered in the analysis of  $E(T_{w,3})$  in Model 2.

In contrast, in Model 3, we eliminated the above assumption on the dependence between  $B_k$  and  $B_{k+1}$ , and assumed that  $B_{k+1}$  is independent from  $B_k$  for  $k = 1, 2, \dots, n_c - 1$  because it is expected that inflow and outflow of mobile nodes weaken the dependence. In addition to this assump-

tion, in Model 3, we added  $P_{turn} \frac{E(\min(Z_{u_2}, Z_{u_3}))}{v}$  to  $E(T_{w,3,k})$  for  $k = 2, 3, \dots, n_c$  as a negative factor of inflow and outflow of mobile nodes. From comparison between numerical results of the analysis and simulation results, we can see that our analysis well approximates  $E(T_{w,3})$  in Model 3. This result indicates that we have two important factors in Model 3. One is that we can consider that  $B_k$  and  $B_{k+1}$  are independent for  $k = 1, 2, \dots, n_c - 1$ . The other is that  $P_{turn} \frac{E(\min(Z_{u_2}, Z_{u_3}))}{v}$  increases the mean waiting time. Also, we can analyze  $E(T_{w,3})$  in Model 3 more simply than in Model 2 because we can compute  $E(T_{w,3,k})$  independently.

The above results give some insights to know what factors affect  $E(T_{w,3})$  in Models 2 and 3. Furthermore, the next step of this research will be understanding behavior of  $E(T_{w,3})$  in more complicated networks like lattice street networks. To analyze  $E(T_{w,3})$  in the complicated networks, we need to consider more complicated problems; however, it is expected that network structures in Models 2 and 3 will appear as parts of such complicated networks, and the above facts that indicate what affects  $E(T_{w,3})$  in Models 2 and 3 will play a fundamental role to understand behavior of  $E(T_{w,3})$  in the complicated networks, and the equations derived in this paper will be applied to the analysis of  $E(T_{w,3})$  in the complicated networks.

## 6. Conclusions

In this paper, we considered delivery of a message M from a source S to a destination D, and analyzed the mean of the minimum waiting time needed for delivery of M. First, we analyzed the mean waiting time in a one-dimensional network consisting of mobile nodes moving along a line. We proposed an approximate method to compute the mean minimum waiting time by using the velocity of flow of M along the line, and showed that this method gave a good approximation to the mean of the minimum waiting time. Second, we modified the approximate method to compute the mean waiting time in a case where shadowing occurs at corners. Using the modified method, we showed how much the mean waiting time is increased by shadowing. Third, we considered another case where mobile nodes change their directions at the corners in addition to shadowing, and approximately analyzed the mean of the minimum waiting time in this case. From the results of this analysis, we showed how much the mean waiting time is increased by the change of direction at the corners. Also, from the results of theoretical analyses, we showed what factors affect the mean waiting time in the last two cases. Extensions of the approximate methods to other models are considered as future works.

## Acknowledgments

This work was partially supported by the Ministry of Education, Science, Sports and Culture, Grant-in-Aid (19560373). The authors would like to thank anonymous reviewers for their valuable comments.

## References

- [1] K. Nakano, K. Miyakita, M. Sengoku, and S. Shinoda, "Analysis and relative evaluation of connectivity of a mobile multi-hop network," IEICE Trans. Commun., vol.E91-B, no.6, pp.1874–1885, June 2008.
- [2] C.E. Perkins, Ad Hoc Networking, Addison-Wesley, 2001.
- [3] K. Mase, K. Nakano, M. Sengoku, and S. Shinoda, "Ad Hoc Networks," J. IEICE, vol.84, no.2, pp.127–134, Feb. 2001.
- [4] P. Santi, "Topology control in wireless ad hoc and sensor networks," ACM Comput. Surv., June 2005.
- [5] R. Groenevelt, E. Altman, and P. Nain, "Relaying in mobile ad hoc networks: The Brownian motion mobility model," Wirel. Netw., vol.12, no.5, Oct. 2006.
- [6] A. Vahdat and D. Becker, "Epidemic routing for partially connected ad hoc networks," Technical Report, Duke University, April 2000.
- [7] S. Hasegawa, Y. Sakumoto, M. Wakabayashi, H. Ohsaki, and M. Imase, "Delay performance analysis on ad-hoc delay tolerant broadcast network applied to vehicle-to-vehicle communication," IEICE Trans. Commun., vol.E92-B, no.3, pp.728–736, March 2009.
- [8] J.F.C. Kingman, Poisson Processes, Oxford University Press, 1993.
- [9] P. Hall, Introduction to the Theory of Coverage Processes, John Wiley & Sons, 1988.
- [10] A. Papoulis and S.U. Pillai, Probability, Random Variables and Stochastic Processes, McGraw-Hill, 2002.

## Appendix A: $X_{fwd}$

The mean of  $x(u_{k+1}, \tau_b) - x(u_k, \tau_b)$  is equal to  $\frac{1}{\lambda} - \frac{r}{e^{\lambda r} - 1}$  for  $k = 0, 1, \dots, M_1 - 1$ , because  $x(u_{k+1}, \tau_b) - x(u_k, \tau_b)$  is exponentially distributed with intensity  $\lambda$  given that it is not longer than  $r$ . Then

$$\begin{aligned} E(X_{fwd,w}) &= \sum_{m_2=0}^{\infty} \sum_{m_1=m_2+1}^{\infty} P(M_1 = m_1, M_2 = m_2 | M_1 > M_2) \\ &\quad \times \left\{ r + (m_1 - m_2) \left( \frac{1}{\lambda} - \frac{r}{e^{\lambda r} - 1} \right) \right\} \\ &= \frac{e^{\lambda r}}{\lambda} - \frac{r}{e^{\lambda r} - 1}, \end{aligned} \quad (\text{A.1})$$

where  $P(M_1 = m_1, M_2 = m_2 | M_1 > M_2)$  can be computed from

$$P(M_1 = m_1) = (1 - e^{-\lambda r})^{m_1} e^{-\lambda r}, \quad (\text{A.2})$$

$$\begin{aligned} P(M_2 = m_2 | M_1 = m_1) &= \begin{cases} \frac{1}{2^{m_2+1}}, & (m_2 \leq m_1 - 1), \\ \frac{1}{2^{m_1}}, & (m_2 = m_1), \end{cases} \end{aligned} \quad (\text{A.3})$$

$$\begin{aligned} P(M_1 > M_2) &= \sum_{m_2=0}^{\infty} \sum_{m_1=m_2+1}^{\infty} P(M_1 = m_1, M_2 = m_2) \\ &= \frac{e^{\lambda r} - 1}{e^{\lambda r} + 1}. \end{aligned} \quad (\text{A.4})$$

From the above equations,

$$\Delta X_{fwd} = \frac{e^{\lambda r} - 1 - \lambda r}{\lambda(e^{\lambda r} + 1)}. \quad (\text{A.5})$$

An inequality  $\Delta X_{fwd} \leq r$  can be rewritten as

$$h(\lambda) = \lambda r e^{\lambda r} + 2\lambda r - e^{\lambda r} + 1 \geq 0. \quad (\text{A} \cdot 6)$$

This holds for  $\lambda \geq 0$  because  $h(0) = 0$  and  $\frac{dh(\lambda)}{d\lambda} = \lambda r^2 e^{\lambda r} + 2r \geq 0$  if  $\lambda \geq 0$ . Therefore,  $\Delta X_{fwd} \leq r$  for  $\lambda \geq 0$ .

### Appendix B: Density Function of $Y$ in Model 1

For  $y \leq r$ , we have  $f_Y(y|C) = 0$  obviously. From Bayes' theorem [10],

$$f_Y(y|C) = \frac{P(C|Y=y)f_Y(y)}{\int_0^\infty P(C|Y=y)f_Y(y)dy}. \quad (\text{A} \cdot 7)$$

In Model 1,  $f_Y(y) = \frac{1}{2}e^{-\frac{1}{2}y}$  because  $Y$  is an exponential random variable with intensity  $\frac{1}{2}$ . Also,

$$P(C|Y=y) = 1 - P_c\left(y, \frac{\lambda}{2}, r\right), \quad (\text{A} \cdot 8)$$

where  $P_c\left(y, \frac{\lambda}{2}, r\right)$  is the probability that  $w_j$  and  $w_{j+1}$  are connected by a multi-hop path consisting of nodes of  $N_b$  given that  $Y = y$ , and can be computed by Eq. (A.1) in [1]. From these equations, we can compute  $f_Y(y|C)$  for  $y \geq r$ . Also, we can compute  $P(C)$  as

$$P(C) = \int_0^\infty P(C|Y=y)f_Y(y)dy. \quad (\text{A} \cdot 9)$$

### Appendix C: Density Function of $T_{walk,k}$

For  $k = 1, 2, \dots, n_c - 1$ ,

$$f_{T_{walk,k}}(t) = \int_{-\infty}^\infty f_{T_{walk}}(t|Y_k=y)f_{Y_k}(y|Y_k \leq a, C_k)dy. \quad (\text{A} \cdot 10)$$

$$f_{T_{walk,n_c}}(t) = \int_{-\infty}^\infty f_{T_{walk}}(t|Y_{n_c}=y)f_{Y_{n_c}}(y|C_{n_c})dy. \quad (\text{A} \cdot 11)$$

For  $y \leq r$  or  $y > a$ , we have  $f_{Y_k}(y|Y_k \leq a, C_k) = 0$  obviously. By Bayes' theorem and some calculations,

$$\begin{aligned} & f_{Y_k}(y|Y_k \leq a, C_k) \\ &= \frac{P(C_k|Y_k=y)f_{Y_k}(y)}{\int_0^a P(C_k|Y_k=y)f_{Y_k}(y)dy} \end{aligned} \quad (\text{A} \cdot 12)$$

for  $k = 1, 2, \dots, n_c - 1$ . As  $f_{Y_{n_c}}(y|C_{n_c})$ , we can use Eq. (A.7). Also, we can compute  $P(C_k|Y_k=y)$  by Eq. (A.8) for  $k = 1, 2, \dots, n_c$ . Also, for  $k = 1, 2, \dots, n_c - 1$ ,

$$P(C_k|Y_k \leq a) = \int_0^a P(C_k|Y_k=y)f_{Y_k}(y|Y_k \leq a)dy. \quad (\text{A} \cdot 13)$$

$$P(C_{n_c}) = \int_0^\infty P(C_{n_c}|Y_{n_c}=y)f_{Y_{n_c}}(y)dy. \quad (\text{A} \cdot 14)$$

$f_{Y_1}(y)$  is identical to  $f_Y(y)$  for Model 1; however,  $f_{Y_k}(y)$  is slightly different from  $f_Y(y)$  for  $k = 2, 3, \dots, n_c$ . Consider Fig. A.1, which shows a typical situation in Model 2. In

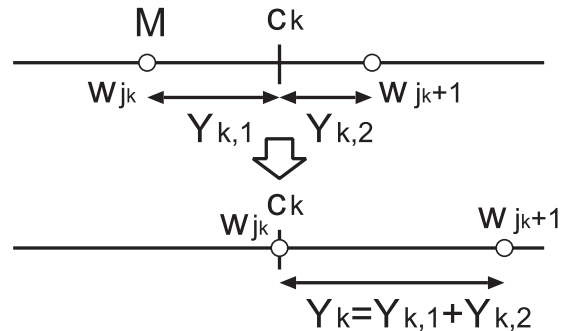


Fig. A.1 Relation between  $w_{jk}$  and  $w_{jk+1}$  in Model 2.

this figure,  $w_{jk}$  is  $n_{h,w}^t$  and has to walk until arriving at  $c_k$  because there is no node of  $N_w$  between  $w_{jk}$  and  $c_k$ . Then, the distance between  $w_{jk}$  and  $c_k$  affects  $Y_k$  in Model 2. Let  $Y_{k,1}$  and  $Y_{k,2}$  be the distance between  $w_{jk}$  and  $c_k$  and that between  $c_k$  and  $w_{jk+1}$  in the situation of the above figure, respectively. Then,  $Y_k$  is  $Y_{k,1} + Y_{k,2}$ . We assume that  $Y_{k,1}$  and  $Y_{k,2}$  are exponential random variables with intensity  $\frac{1}{2}$ .

Then, the density function of  $Y_{k,1}$  is  $f_{Y_{k,1}}(y) = \frac{\frac{1}{2}e^{-\frac{1}{2}y}}{1 - e^{-\frac{1}{2}a}}$  because  $Y_{k,1}$  must be smaller than or equal to  $a$  because  $w_{jk}$  is in  $I_{k-1}$ . Also, the density function of  $Y_{k,2}$  is  $f_{Y_{k,2}}(y) = \frac{1}{2}e^{-\frac{1}{2}y}$ . Then,

$$f_{Y_k}(y) = f_{Y_{k,1}+Y_{k,2}}(y) = \frac{\lambda^2 y e^{\frac{1}{2}(a-y)}}{4(e^{\frac{1}{2}a} - 1)}. \quad (\text{A} \cdot 15)$$

Note that  $E(Y_{k,1}) = \frac{2}{\lambda} - \frac{a}{e^{\frac{1}{2}a} - 1}$  for  $2 \leq k \leq n_c$ .



**Keisuke Nakano** received B.E., M.E. and Ph.D. degrees from Niigata University in 1989, 1991 and 1994, respectively. He is currently an Associate Professor of the Department of Information Engineering at Niigata University. He received the Best Paper Award of IEEE IC-NNSP'95. He also received the Best Paper Award of IEICE in 1997. He was a visiting scholar at the University of Illinois in 1999. His research interests include computer and mobile networks. He is a member of IEEE.



student member of IEEE.

**Kazuyuki Miyakita** graduated from the advanced engineering course of Nagaoka National College of Technology, and received the B.E. and M.E. degrees from National Institution of Academic Degrees in 2005 and Niigata University in 2007, respectively. He is a Ph.D. candidate of Graduate School of Science and Technology, Niigata University. He received the Young Researcher Paper Award of IEEE Shintetsu Section in 2008, and the Student Presentation Award of IEICE CAS in 2009. He is a



**Akira Otsuka** received B.E. and M.E. degrees from Niigata University in 1985 and 1987, respectively. He is currently with Information Technology R&D Center, Mitsubishi Electric Corporation.



**Masakazu Sengoku** received a B.E. degree from Niigata University in 1967 and M.E. and Ph.D. degrees from Hokkaido University in 1969 and 1972, respectively. He is a Professor in the Department of Information Engineering at Niigata University. His research interests include network theory, graph theory, and mobile communications. He received the Best Paper Awards of IEICE in 1992, 1996, 1997 and 1998, the Achievement Award of IEICE in 2005, and the Distinguished Achievement and Contributions Award in 2009. He also received the Best Paper Award of the 1995 IEEE ICNNSP. He is a fellow of the IEEE.

He also received the Best Paper Award of the 1995 IEEE ICNNSP. He is a fellow of the IEEE.



**Shoji Shinoda** received B.E., M.E. and D.E. degrees, all in electrical engineering, from Chuo University, Tokyo, Japan, in 1964, 1966, and 1973, respectively. In April, 1965, he joined the Faculty of Science and Engineering at Chuo University, Tokyo, Japan. Since then, he has engaged in education and research in the fields of electrical circuit theory, network flow and tension theory, discrete systems, and mobile communication systems. He is now a Professor in the Department of Electrical, Electronic and

Communication Engineering at Chuo University. He has published more than one hundred technical papers in these fields. He is also the recipient of the 1992 IEICE Best Paper Award, the 1997 IEICE Best Paper Award, the 1998 IEICE Best Paper Award, the Best Paper Award of the 1995 IEEE International Conference on Neural Networks and Signal Processing, the 2005 IEICE Achievement Award, and the 2007 Distinguished Achievement and Contributions Award. He is now a fellow of the IEEE and a member of the Society of Instrument and Control Engineers, the Japan Society of Simulation Technology, and the Korean Institute of Telematics and Electronics.